ANNUAL REVIEWS

Annual Review of Fluid Mechanics

Spontaneous Aggregation of Convective Storms

Caroline Muller,[1,14] Da Yang,[2,3] George Craig,[4] Timothy Cronin,[5] Benjamin Fildier,[1] Jan O. Haerter,[6,7,8] Cathy Hohenegger,[9] Brian Mapes,[10] David Randall,[11] Sara Shamekh,[12] and Steven C. Sherwood[13]

[1]Laboratoire de Météorologie Dynamique, CNRS UMR 8539, Institut Pierre Simon Laplace, Ecole Normale Supérieure, Université Paris Sciences et Lettres, Paris, France; email: carolinemuller123@gmail.com

[2]Department of Land, Air and Water Resources, University of California, Davis, California, USA

[3]Lawrence Berkeley National Laboratory, Berkeley, California, USA

[4]Deutsches Zentrum für Luft und Raumfahrt, Munich, Germany

[5]Massachusetts Institute of Technology, Cambridge, Massachusetts, USA

[6]Niels Bohr Institute, Copenhagen University, Copenhagen, Denmark

[7]Complexity and Climate Research Group, Leibniz Center for Tropical Marine Research, Bremen, Germany

[8]Department of Computer Science and Electrical Engineering, Jacobs University, Bremen, Germany

[9]Max Planck Institute for Meteorology, Hamburg, Germany

[10]Department of Atmospheric Sciences, University of Miami, Miami, Florida, USA

[11]Department of Atmospheric Science, Colorado State University, Fort Collins, Colorado, USA

[12]Department of Earth and Environmental Engineering, Columbia University, New York, NY, USA

[13]ARC Centre of Excellence for Climate Extremes, University of New South Wales, Sydney, Australia

[14]Current affiliation: Institute of Science and Technology Austria, Klosterneuburg, Austria

Annu. Rev. Fluid Mech. 2022. 54:133–57

First published as a Review in Advance on September 23, 2021

The *Annual Review of Fluid Mechanics* is online at fluid.annualreviews.org

https://doi.org/10.1146/annurev-fluid-022421-011319

Keywords

deep convection, self-aggregation, radiative–convective equilibrium, convective organization, Madden–Julian oscillation, precipitation extremes, climate sensitivity, tropical cyclones

Abstract

Idealized simulations of the tropical atmosphere have predicted that clouds can spontaneously clump together in space, despite perfectly homogeneous settings. This phenomenon has been called self-aggregation, and it results in a state where a moist cloudy region with intense deep convective

storms is surrounded by extremely dry subsiding air devoid of deep clouds. We review here the main findings from theoretical work and idealized models of this phenomenon, highlighting the physical processes believed to play a key role in convective self-aggregation. We also review the growing literature on the importance and implications of this phenomenon for the tropical atmosphere, notably, for the hydrological cycle and for precipitation extremes, in our current and in a warming climate.

1. INTRODUCTION

Convective organization: long-lived and upscale-growing convective systems that cover an area larger than the individual convective cells, typically a few kilometers

Self-aggregation: spontaneous, unforced emergence of convective organization that persists for much longer than an individual cloud (~1 to a few hours) and usually longer than the anvil cloud lifetime (many hours)

Cloud-resolving model (CRM): a computer model that solves the governing equations at kilometer-scale horizontal resolution and that is capable of explicitly simulating deep convective clouds

Radiative–convective equilibrium (RCE): a statistical energy equilibrium between convective heating and radiative cooling in the atmosphere

Few geophysical phenomena are as spectacular as tropical cyclones, a form of convective organization spanning hundreds of kilometers. Their eyes, devoid of deep clouds, are surrounded by a sharp cloudy eyewall whose rotating winds are among the strongest on our planet. There are other types of organized deep convection. Convection is the overturning of air within which clouds are embedded [clouds are found in ascending regions; see Stevens (2005) for a review on moist convection], and deep convection is convection spanning the whole depth of the troposphere, as is the case for tropical cyclones. In fact, the organization of deep convection at mesoscales, i.e., hundreds of kilometers, is ubiquitous in the tropics (Houze 2004).

Convective organization can be forced by large scales (i.e., scales similar to or larger than mesoscales), e.g., vertical wind shear (Muller 2013), land–ocean contrasts (Cronin et al. 2015), or circulation such as that associated with the passage of large-scale equatorial waves (Kiladis et al. 2009). However, in the tropics, these alone cannot explain the organization of all convective systems since wind shear is often too weak, upscale growth is ubiquitous and sometimes rapid, and convective inhibition is small, especially over tropical oceans, so small perturbations can easily initiate new convection.

Organization can also arise from internal feedback loops linked to the interaction of clouds with their environment, leading to the spontaneous inhomogeneous spatial clustering of clouds in otherwise homogeneous unforced environments, e.g., self-organization by small-scale gravity waves excited by the convection, which destabilize the near-cloud environment and promote new convection (Mapes 1993). Organization can also arise from so-called internal self-aggregation feedback loops, which are still very much an area of active research (for a recent review, see, e.g., Wing et al. 2017).

The topic of this review is self-aggregation—the spectacular ability of deep clouds to spontaneously cluster in space despite homogeneous boundary conditions and forcing (**Figure 1*b***). We limit ourselves to tropical deep storms that are strong enough to span the troposphere (roughly 15 km); pattern formation in stable boundary layer clouds presents another vast and fascinating problem (Wood 2012). Some of the fundamental scales for tropical deep convection are given in **Table 1** below.

Since the seminal paper of Held et al. (1993) showing the localization of convection in a 2D cloud-resolving model (CRM; see margin definition), a rapidly growing body of literature on self-aggregation has confirmed its occurrence in a hierarchy of models and settings, from 2D and 3D CRMs to regional and global climate models (GCMs) with parameterized clouds and convection, with superparameterized clouds and convection, or without a convective parameterization. Key results from those numerical studies have recently been reviewed (Wing et al. 2017, Wing 2019). Therefore, here we instead focus on key results from idealized simulations [namely radiative–convective equilibrium (RCE); see margin definition], and from theoretical and conceptual models. We mainly focus on convection in tropical conditions and thus ignore the

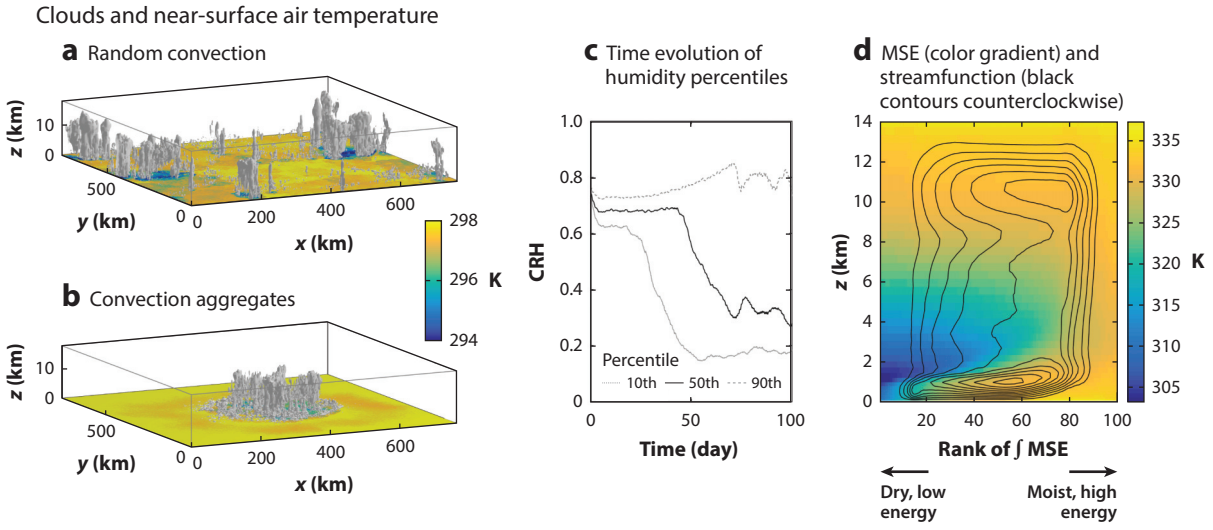

Figure 1

In models, randomly distributed moist convection (*a*) can spontaneously organize in space (*b*), even in idealized settings without any heterogeneity or large-scale forcing (Bretherton et al. 2005). (*c*) The time evolution of CRH percentiles in the aggregated simulation shown in panel *b*. CRH is the ratio of the precipitable water to the saturation water vapor path. Self-aggregation is associated with an overall drying of the atmosphere with enhanced humidity variance, which initially is due to significantly drier conditions in dry regions and slightly moister conditions in moist regions. (*d*) The pointwise MSE (*color gradient*) and the circulation streamfunction (*black contour lines*) in the aggregated simulation in panel *b* as a function of height and vertically integrated (i.e., $\int \mathrm{MSE}\rho\, dz$; see **Table 2** for acronyms and notations used in this review). Self-aggregation is associated with a shallow flux (below ~1 km) from dry, low-energy regions to moist, high-energy regions. Figure adapted with permission from Muller & Held (2012); copyright 2012 American Meteorological Society. Abbreviations: CRH, column-relative humidity; MSE, moist static energy.

earth's rotation, which is a reasonable approximation close to the equator (we discuss the effects of rotation in Section 4).

We first briefly review results from full-physics simulations in idealized settings (Section 2). Then, the core of this paper reviews four theoretical and conceptual models that have been

Table 1 Scales for tropical deep convection

Description	Scale
Spatial scales	
Vapor mass scale height	~3 km
Radiative troposphere depth	~14 km
Cloud base for oceanic conditions	~700 m
Single cloud	~1 km
Mesoscale complex	~100 km
Velocity scales	
Updraft speed ~ water drop fall speed	$w_u \sim 7$ m/s
Clear-air descent rate	$w_d \sim 1$ cm/s
Internal wave speed (for vertical mode n)	$\sim 50/n$ m/s
Timescales	
Single-cloud lifetime	~1 h
Mesoscale complex lifetime	Days

proposed to simulate and understand deep moist convective self-aggregation (Section 3). Each model emphasizes different physics, including atmospheric radiation, turbulent entrainment at the edge of clouds, gravity waves, and cold pools—regions of cold air below precipitating clouds (visible, e.g., in **Figure 1*a***) due to latent cooling from the partial evaporation of rain. We end with a discussion of implications of self-aggregation for earthly deep convective phenomena (Section 4), followed by concluding remarks and outstanding questions (Section 5).

2. SELF-AGGREGATION IN IDEALIZED NUMERICAL SIMULATIONS: DIAGNOSTIC FRAMEWORKS

In this section, we briefly review the key findings from numerical studies of self-aggregation. We start by describing the models and qualitative analysis of the key physical processes in sensitivity simulations. We notably describe the key role of radiatively induced shallow circulations from dry to moist regions (Section 2.1). Then, we introduce the main diagnostics used to analyze simulations, which are aimed at quantifying the contributions from diabatic terms, including radiation (Section 2.2), and from boundary layer buoyancy anomalies (Section 2.3).

2.1. Sensitivity Simulations Removing Specific Physical Processes

Self-aggregation was first discovered in CRMs (as in **Figure 1*a*,*b***) over constant sea surface temperature (SST) (more complex surfaces will be discussed in Section 4.1) in idealized settings, namely, nonrotating RCE. Such CRMs typically solve the momentum, mass, energy, and water conservation equations, which are given by, e.g., Khairoutdinov & Randall (2003),

$$\frac{\mathrm{D}\mathbf{u}}{\mathrm{D}t} = -\nabla\frac{p}{\rho_0} + b\mathbf{z} + F^{\mathbf{u}}, \qquad 1.$$

$$\nabla\cdot(\rho_0\mathbf{u}) = 0, \qquad 2.$$

$$\frac{1}{\theta_0}\frac{\mathrm{D}\theta}{\mathrm{D}t} + \frac{w}{\theta_0}\frac{\mathrm{d}\theta_0}{\mathrm{d}z} = \frac{1}{c_\mathrm{p}T}(\dot{\theta}_\mathrm{rad} + L_\mathrm{v}\dot{r}_\mathrm{l} + \dot{\theta}_\mathrm{sfc}) + F^{\theta}, \qquad 3.$$

$$\frac{\mathrm{D}r}{\mathrm{D}t} = -\dot{r}_\mathrm{l} + \dot{r}_\mathrm{sfc} + F^{r}, \qquad 4.$$

where $\mathrm{D}/\mathrm{D}t$ is the total Lagrangian derivative, $\mathbf{u}$ is the velocity vector (u, v, w), ρ is the density perturbation from a reference profile ρ_0 that depends on altitude z, θ is the potential temperature anomaly from a reference profile θ_0 ($\mathrm{d}\theta_0/\mathrm{d}z$ is the mean stratification), $b = -g\rho/\rho_0$ ($\approx g\theta/\theta_0$) is the buoyancy perturbation associated with density perturbation ρ, p is the pressure, T is the absolute temperature, L_v is the latent heat of vaporization, c_p is the isobaric specific heat capacity of air, $\dot{\theta}_\mathrm{rad}$ is the radiative heating [including long wave, which is primarily infrared, and short wave, which is primarily visible (e.g., Pierrehumbert 2010)], $F^{(...)}$ are subgrid-scale fluxes, $(...)_\mathrm{sfc}$ are surface fluxes, and, for simplicity, water is assumed to have two phases, vapor and liquid, with mixing ratios r and r_l, respectively (otherwise, the latent heat associated with ice transition would also appear). For simplicity, we neglect the buoyancy effect of water vapor due to its molecular weight being smaller than dry air (Yang 2018a, Yang & Seidel 2020). Vapor buoyancy affects b, $\dot{\theta}_\mathrm{rad}$ (Seidel & Yang 2020), and, thereby, the development and size of convective aggregation. Readers are referred to Yang (2018a,b) and Shamekh et al. (2020a) for details. Note that both the radiative and the surface diabatic terms are functions of the local thermodynamic conditions (temperature, humidity, and condensate amounts) and, thus, interact with convection.

Combining Equations 3 and 4 and neglecting subgrid and surface fluxes, we see that under adiabatic displacements this system has an approximately conserved variable, the equivalent potential

temperature, $\theta_e = (\theta + \theta_0) \exp[L_v r/(c_p T)]$. This is equivalent to the (approximate) conservation of $c_p T + gz + L_v r$, termed moist static energy (MSE) (e.g., Muller 2019). MSE is thus the relevant energy for moist convection, as it is conserved during moist adiabatic processes, including the phase change of water.

An emerging consensus across models is that radiative feedback loops are key for long-lived self-aggregation, in particular for long-wave radiative feedback loops (Bretherton et al. 2005, Muller & Held 2012). More precisely, strong long-wave radiative cooling in dry regions, from both clear-sky and shallow clouds, and reduced radiative cooling in moist regions covered by high clouds (which trap outgoing long-wave radiation emitted to space by the surface and low troposphere) result in a differential cooling between dry and moist regions. This differential cooling generates a circulation at low levels (below ~2 km; **Figure 1*d***). The cooling in dry regions yields subsidence, reduced cooling (or even heating) in moist regions yields upward motion, and between the two there is a near-surface flow (below ~1 km) from dry to moist regions. This flow transports MSE from dry to moist regions (i.e., upgradient, which is believed to maintain the self-aggregation) (Bretherton et al. 2005, Muller & Bony 2015, Sessions et al. 2016). Consistently, mechanism-denial simulations show that homogenizing radiation at low levels suppresses self-aggregation (**Figure 2**).

Another feedback affecting self-aggregation is the moisture feedback, related to turbulent entrainment at the edge of clouds in the moist region. Cloudy updrafts entrain neighboring air at their edge, which decreases their buoyancy and upward motion (through drying and evaporatively driven latent cooling). With self-aggregation, the air surrounding updrafts is relatively moist, reducing the negative effect of entrainment and favoring the clustering of updrafts in the moist region (Grabowski & Moncrieff 2004, Tompkins & Semie 2017).

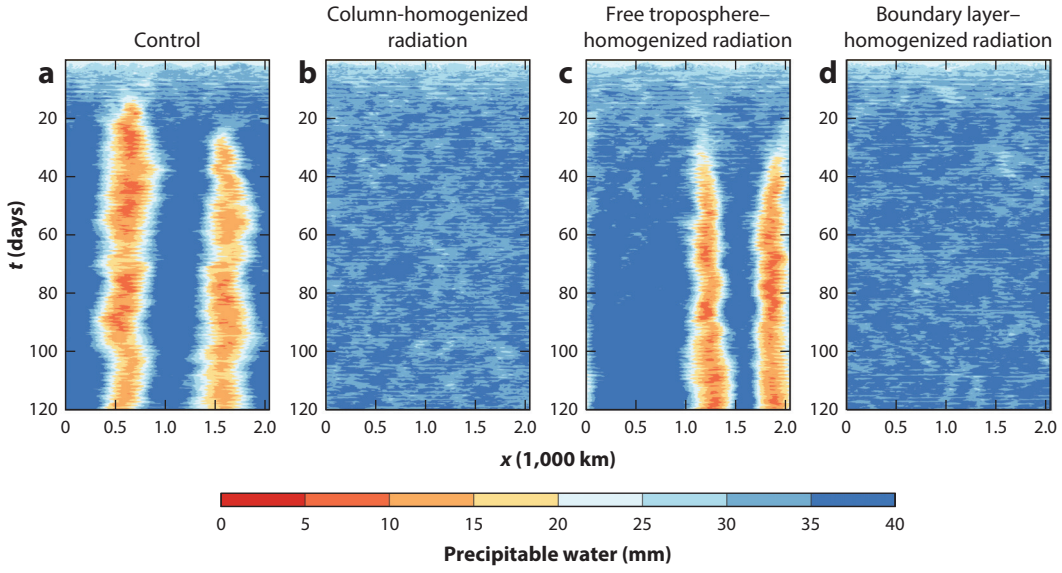

Figure 2

Sensitivity experiments in 2D cloud-resolving model simulations: Hovmöller diagrams of precipitable water in the control simulation (*a*) and in simulations with horizontally homogenized radiative cooling rates for the entire column (*b*), for the free troposphere (*c*), and for the boundary layer (*d*). Similar experiments have been performed using 3D experiments [e.g., Muller & Bony (2015); see also **Supplemental Video 1**]. Figure adapted with permission from Yang (2018a).

Supplemental Material >

The properties of self-aggregation are somewhat sensitive to the model used, as well as the resolution, domain size, and subgrid parameterizations, notably the microphysics and radiation (e.g., Muller & Held 2012). It typically takes $\mathcal{O}$(10 days) for convective self-aggregation to emerge with constant SST and constant incoming solar radiation. What controls this timescale for self-aggregation? Changing the surface conditions, or including diurnal variations of the solar flux, can also significantly slow down or accelerate the self-aggregation process, for reasons that are not fully understood (see Section 4.1 for more details).

At steady state, the typical horizontal scale of self-aggregation λ is of $\mathcal{O}$(2,000 km). In domain sizes less than 5,000 km^2, a single moist cluster forms, covering ~20–25% of the domain, but larger domains can accommodate multiple convective clusters (Arnold & Putman 2018, Patrizio & Randall 2019). Quantitative theories have been developed to explain the spatial scale of aggregation. Wing & Cronin (2016) proposed that λ linearly scales with the boundary layer height, which monotonically decreases with surface warming. However, λ varies with SST nonmonotonically (Yang 2018b). Yang (2018b) then proposed that the boundary layer height and buoyancy variation within the boundary layer together determine λ (see Section 3.4 and Equation 13 for more details), which was applied to explain large-domain simulations (Arnold & Putman 2018, Patrizio & Randall 2019). Although the two theories differ in details, they both point to the importance of the boundary layer in controlling the spatial scale of self-aggregation.

2.2. Moist Static Energy Analysis (Including Moist Static Energy Transport by Circulation)

Self-aggregation is associated with an increase in the spatial variance of vertically integrated $\widehat{\mathrm{MSE}}$ (see **Table 2** for notations), as moist regions become moister and dry regions become drier (**Figure 1*c***). One way to quantify the contribution of various feedback loops to self-aggregation is thus to quantify their contribution to the increase in the $\widehat{\mathrm{MSE}}$ variance.

This can be done using the $\widehat{\mathrm{MSE}}$ variance budget (Wing & Emanuel 2014),

$$\frac{\mathrm{d}(\widehat{\mathrm{MSE}}')^2}{\mathrm{d}t} = \widehat{\mathrm{MSE}}' F'_{\mathrm{sfc}} + \widehat{\mathrm{MSE}}' \widehat{\theta}'_{\mathrm{rad}} - \widehat{\mathrm{MSE}}' C_{\mathrm{h}}, \qquad 5.$$

where the hat symbol denotes the mass-weighted integral (see **Table 2** for notations), the prime symbol denotes a departure from the domain mean, F_{sfc} is the total surface enthalpy flux (latent plus sensible), $\widehat{\theta}_{\mathrm{rad}}$ is the total net radiative heating (short wave plus long wave, which is obtained

Table 2 Acronyms and notations

Abbreviation	Definition
RCE	Radiative–convective equilibrium
MSE	Moist static energy
SST	Sea surface temperature
$\widehat{X}$	Mass-weighted vertical integral: $\widehat{X} = \int X \rho \, \mathrm{d}z \approx \int X \, \mathrm{d}p/g$ (from hydrostasy)
CRM	Cloud-resolving model
APE	Available potential energy
GCM	Global climate model
ITCZ	Intertropical Convergence Zone
ECS	Equilibrium climate sensitivity

by vertically integrating $\dot{\theta}_{\mathrm{rad}}$ in Equation 3), C_{h} is the horizontal MSE advection, and we have neglected subgrid-scale fluxes (other than surface fluxes).

This equation allows one to quantify the feedback loops from diabatic terms (surface and radiative fluxes) on self-aggregation. For instance, the first term on the right-hand side is positive if surface fluxes are anomalously large in high-energy regions, strengthening the $\widehat{\mathrm{MSE}}$ variance and yielding a positive feedback loop. In idealized simulations with homogeneous and fixed SSTs, surface fluxes are found to favor self-aggregation at its early stage, as enhanced wind speed in convective regions increases the surface fluxes, known as WISHE (wind-induced surface heat exchange), which in return favors convection locally and creates a positive feedback loop. Once self-aggregation is well established, increased surface–air moisture disequilibrium in nonconvective regions enhances the surface fluxes there, thus reducing the variance of $\widehat{\mathrm{MSE}}$, which acts against the maintenance of self-aggregation (Wing & Emanuel 2014). Similarly, anomalous radiative cooling in dry low-$\widehat{\mathrm{MSE}}$ regions weakens the $\widehat{\mathrm{MSE}}$ there, strengthening the $\widehat{\mathrm{MSE}}$ variance and yielding a positive feedback loop on self-aggregation. This framework thus allows one to compare the strength of the various diabatic feedback loops, and results from such analyses have highlighted the sensitivity of the dominating aggregating feedback loop to SST (Wing & Cronin 2016).

In addition to those direct diabatic feedback loops, diabatic terms induce circulations whose MSE transport is believed to be key to the development of aggregation (included in the last term of Equation 5). A potential metric to capture the MSE transport is the strength of the shallow circulation (related to the maximum of the streamfunction at low levels; **Figure 1*d***) compared to the overall circulation strength (deep and shallow) (Shamekh et al. 2020a). Indeed, MSE is a strong function of height (with high MSE near the surface and at high altitudes with a minimum in the mid-troposphere), and a shallow circulation will export near-surface high MSE from dry regions and import mid-level low MSE into dry regions, yielding a net export of MSE from dry regions. This yields a positive feedback loop on self-aggregation (Bretherton et al. 2005, Raymond et al. 2009). A deep circulation, in contrast, imports very high MSE from high altitudes into dry regions (upper branch of the circulation; **Figure 1*d***), yielding a net import of MSE into dry regions and a negative feedback loop on self-aggregation. Several processes can give rise to this shallow circulation (including radiation, but also moisture effects), but the shallow circulation and concomitant MSE transport seem to be key to feedback loops supporting self-aggregation. Consistently, the self-aggregation strength is closely related to the shallow circulation strength (**Figure 3**).

2.3. Available Potential Energy Analysis

Another quantity to diagnose the various feedback loops contributing to self-aggregation is the available potential energy (APE). APE is generated and immediately converted to kinetic energy by heated buoyancy updrafts. APE production leads to amplifying waves (Emanuel et al. 1994) and is clearly associated with the development of self-aggregation (Yang 2018a).

In an anelastic atmosphere, the APE is defined as

$$\mathrm{APE} = \frac{1}{2}\int_0^z \frac{\overline{b'^2}}{N^2}\rho_0\,\mathrm{d}z, \qquad 6.$$

where $\rho_0 = \rho_0(z)$ is the reference density, the overbar symbol denotes the horizontal average, the prime indicates departure from this average, b' is buoyancy (which, as noted below Equations 1–4, is related to potential temperature, $b \approx g\theta'/\theta_0$), and $N^2 = N^2(z)$ is the Brunt–Väisälä frequency (also called buoyancy frequency, which is related to the mean stratification in Equation 3:

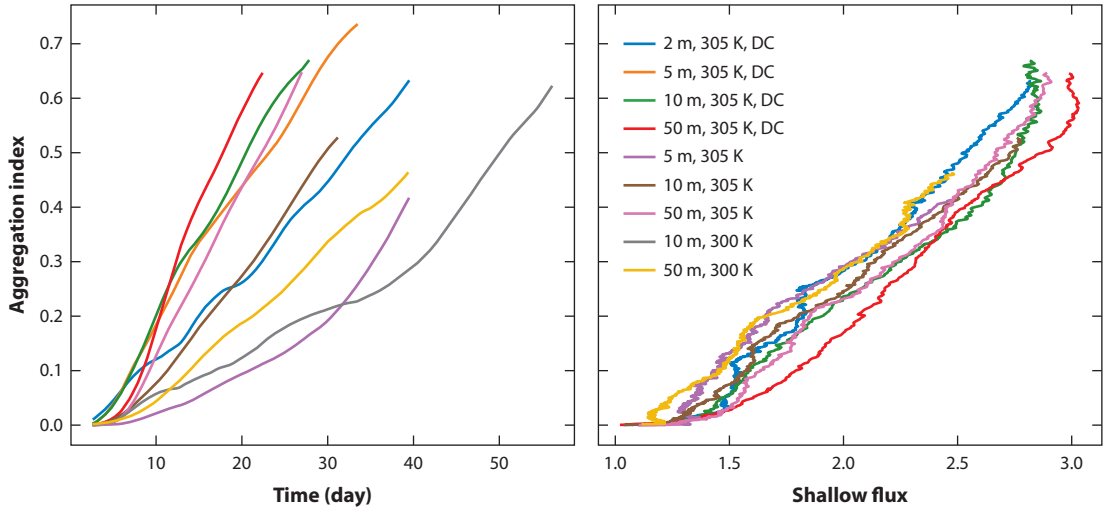

Figure 3

(*Left*) Time evolution of self-aggregation as measured by the spatial variance of column-relative humidity in simulations that vary ocean mixed-layer depth, sea surface temperature (SST), and the inclusion of a diurnal cycle (DC); readers are referred to Shamekh et al. (2020a) for details. (*Right*) Evolution of self-aggregation versus the shallow circulation (measured by the low-level streamfunction maximum). The timescale of self-aggregation can vary greatly between simulations, but when plotted against the strength of the shallow circulation, the curves all fall on top of each other.

$N^2 = g/\theta_0\, d\theta_0/\mathrm{d}z$). The APE budget of self-aggregation (slow component) can be derived from the buoyancy equation and is given by

$$\overbrace{\frac{1}{2}\int_0^z \partial_t \overline{b'^2}\frac{\rho_0 \mathrm{d}z}{N^2}}^{\partial_t \mathrm{APE}} = \overbrace{\int_0^z \overline{b' S_\mathrm{b}'}\frac{\rho_0 \mathrm{d}z}{N^2}}^{\text{Production}} - \underbrace{\int_0^z \overline{b'(u\partial_x b)'}\frac{\rho_0 \mathrm{d}z}{N^2}}_{\text{Advection}} - \underbrace{\int_0^z \overline{b' w'}\rho_0 \mathrm{d}z}_{\text{Conversion}}, \qquad 7.$$

where S_b denotes all diabatic sources of buoyancy (right-hand side of Equation 3). Equation 7 has been used to diagnose CRM simulations. Positive APE production corresponds to amplifying effects and negative values correspond to decaying effects (Emanuel et al. 1994). This suggests that the circulation's powering, as discussed in Sections 2.1 and 2.2 and shown in **Figures 1*d*** and **3**, relies on positive correlations between buoyancy sources and buoyancy anomalies when the atmosphere is stably stratified.

Although a diagnostic framework, this APE analysis has successfully predicted that diabatic processes in the boundary layer (i.e., the lowest 2 km) are key to the development of self-aggregation (Yang 2018a), consistent with mechanism-denial numerical experiments (**Figure 2**). In a slowly or nonrotating atmosphere, there is limited APE production in the free troposphere for large-scale long-lasting circulations. This is because the APE production requires buoyancy anomalies, which are effectively smoothed out by gravity waves in the free troposphere (Sobel et al. 2001). The boundary layer is likely the only part of the atmosphere that can sustain substantial buoyancy anomalies, which are necessary to generate APE.

Although this diagnostic has helped to clarify the key role of boundary layer radiation (**Figure 2**), consistent with the aforementioned importance of the radiatively driven shallow circulation (**Figure 3**), we cannot rule out the role of the free troposphere, notably free-tropospheric drying. Indeed, radiation is nonlocal, and humidity in the free troposphere affects boundary layer

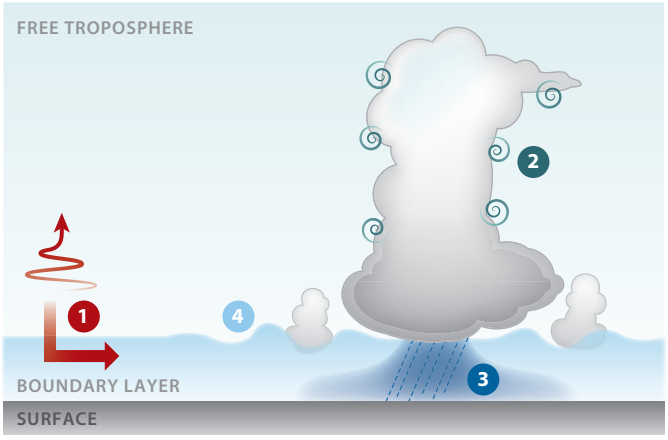

Figure 4

The key physical processes leading to self-aggregation: (❶) enhanced radiative cooling in dry regions and associated shallow divergent circulation (*red arrow*), (❷) turbulent entrainment of environmental air at the edge of clouds, (❸) evaporation-driven cold pools in the boundary layer, and (❹) boundary layer wave emission.

radiative cooling in dry regions, which can amplify the effects of drying, high pressure, or low-level circulations (Shamekh et al. 2020a).

3. SIMPLE MODELS AND FRAMEWORKS: HIERARCHY OF VERTICAL LAYERS, PROCESS COMPLEXITY

In this section, we discuss four groups of simple models that aim at reproducing basic features of self-aggregation. These mathematical models were motivated by results from comprehensive CRM simulations and emphasize the role of different physical processes leading to self-aggregation. These physical processes are illustrated schematically in **Figure 4**. Two models concern column-wise processes, including interactions among water vapor, radiation, and convection. Water vapor interacts with radiation through enhanced radiative cooling in dry regions (process ❶ in **Figure 4**), and water vapor interacts with convection through the entrainment of environmental air at the edge of clouds (process ❷ in **Figure 4**). The other two models consider explicitly dynamical interactions, including cold pools of air and convection–gravity wave interactions. The former involves cold pockets of air driven by the evaporation of rain in precipitating clouds (process ❸ in **Figure 4**), and the latter involves the emission and interaction of boundary layer waves with convection (process ❹ in **Figure 4**). Which process, if any, dominates in our current climate and how the dominating process may change with warming are still unknown and the topics of ongoing research. Regardless of their relevance to observed aggregation, these theoretical models have clarified fundamental ways in which convection interacts with its environment.

3.1. Radiative Instability

As suggested by **Figure 2** and highlighted in both MSE and APE analysis frameworks of self-aggregation, the interaction between radiative heating rates and the humidity of the atmosphere can play a key role in self-aggregation of deep convection. Preferential radiative heating of moist regions relative to dry regions can serve as the basis for a potential instability: Differential heating may drive an overturning circulation with rising air in moist regions and sinking air in dry regions, which further increases the humidity differences between regions due to the decrease in water

vapor with altitude (Raymond 2000, Mapes 2001). Note that this is a similar argument to that concerning the circulation discussed in Section 2.2, but here it is described in terms of moisture transport instead of MSE transport. This instability can proceed until it is balanced by some other mechanism that reduces the humidity contrast between moist and dry regions, such as surface evaporation, lateral mixing, or a reversal of the tendency of moist areas to be radiatively heated more than dry regions (Wing & Emanuel 2014, Beucler & Cronin 2016).

We use the term "radiative instability" to refer to the notion that radiative heating rates covary with column water vapor in a way that amplifies a perturbation from an initially homogeneous state. A straightforward potential condition for radiative instability is that the column-integrated radiative heating $\widehat{\dot{\theta}}_{\mathrm{rad}}$, including long-wave and short-wave contributions, increases with the column-integrated water vapor, $\widehat{r} = \int r \, \mathrm{d}p/g$, or that $\partial \widehat{\dot{\theta}}_{\mathrm{rad}}/\partial \widehat{r}$ is positive (Beucler & Cronin 2016). The characterization of self-aggregation as a linear instability of the tropical atmosphere is a key theoretical goal that we elaborate on below.

Although a moister atmosphere nearly always reduces the upward long-wave flux at the top of the atmosphere, the impact of moistening on the net long-wave radiative heating of an atmospheric column is more subtle because changes in the net surface radiative flux must also be considered. Emanuel et al. (2014) used a two-layer emissivity model, which crudely represented humidity in the upper and lower troposphere, to reason that when the lower troposphere becomes sufficiently optically thick so that its cooling to space depends on humidity in the upper troposphere, the potential instability condition $\partial \widehat{\dot{\theta}}_{\mathrm{rad}}/\partial \widehat{r} > 0$ likely holds. They further hypothesized that this condition was likely to hold only at sufficiently high temperatures, close to those of the present tropical atmosphere or slightly above. Beucler & Cronin (2016) formalized and extended these results, using analytic models with a continuous rather than two-layer vertical coordinate, and found that the vertical structure of water vapor perturbation was a key control on the sign of $\partial \widehat{\dot{\theta}}_{\mathrm{rad}}/\partial \widehat{r}$. The removal or addition of water vapor in the middle and upper troposphere is likely to favor radiative instability ($\partial \widehat{\dot{\theta}}_{\mathrm{rad}}/\partial \widehat{r} > 0$), whereas the removal or addition of water vapor in the lower troposphere is likely to disfavor it ($\partial \widehat{\dot{\theta}}_{\mathrm{rad}}/\partial \widehat{r} < 0$). Calculations that have included clouds, short-wave radiative heating (which always increases with $\widehat{r}$), and more realistic spectroscopy for water vapor all lowered the moisture threshold for radiative instability and confirmed its sensitivity to the vertical structure of the humidity perturbation. By analyzing observations, Beucler & Cronin (2016) also found that the vertical structure of typical humidity variations in the real tropical atmosphere was likely consistent with the radiative instability condition $\partial \widehat{\dot{\theta}}_{\mathrm{rad}}/\partial \widehat{r} > 0$, even when considering only clear-sky radiative heating.

This relatively simple picture of radiative instability is complicated, however, by the coupling between atmospheric radiative heating and the vertical transport of water and heat by moist convection. The evolution of a humidity perturbation is influenced not only by the large-scale circulation associated with the differential radiative heating it induces, but also by the way that smaller-scale convective turbulence might amplify or dissipate that humidity anomaly.

Some beautiful work has been done to distill how convection heats and moistens the atmosphere by constructing linear response functions of an ensemble of convective clouds with small moisture or temperature perturbations at different heights (Kuang 2010, Herman & Kuang 2013). These methods provide some similarities in the linear response of convective heating and moistening, but also are beset by dependencies on domain size and geometry, by unresolved physics and dynamics at the scale of the simulations, and by a lack of observational or experimental ground truth. We also lack comprehensive theoretical models for how moist convective turbulence should be expected to respond to a change in humidity at different heights. Despite these issues, Beucler et al. (2018) attempted to couple linear response models for clear-sky radiative heating with

convective heating and moistening by providing an analysis of the linear stability problem in terms of eigenvalues and eigenvectors of a combined radiative and convective heating linear response matrix. This work demonstrated that a potential radiative instability was not sufficient for unstable eigenmodes, and that radiation and convection can combine to give unstable modes even when neither's response is unstable in isolation. The linear response of convection was found to dominate the vertical structure of humidity anomalies in the most unstable (or least stable) modes in most circumstances. Kuang (2018) used similar approaches to couple convective and radiative linear response functions using a more complex model to generate the convective response matrix. One branch of unstable solutions was found to require radiative feedback loops, which is consistent with the importance of radiative instability.

3.2. Phase Transition and Coarsening

One appealing approach is to describe self-aggregation as a phase transition. This description predicts that the resulting spatial organization will have certain universal properties that are shared by a large class of physical systems. As described in the introduction, the self-aggregation found in simulations of convection takes the form of the emergence of regions of high and low MSE (for simplicity, wet and dry regions) that grow in size over time. This is in some ways reminiscent of phase separation processes like the growth of water droplets in a supersaturated atmosphere or the separation of a mixture of oil and water, both of which are examples of a phenomenon called coarsening (Sethna 2006).

Two conditions must be satisfied for a system to undergo phase separation by coarsening. The systems must have (*a*) a local bistable equilibrium (in the absence of spatial interactions, the system will evolve to one of two preferred states, e.g., wet or dry) and (*b*) local interactions in space (each location interacts only with neighboring regions, e.g., a process such as diffusion rather than a long-range transport that introduces a characteristic length scale).

Perhaps the simplest example of a system that meets these requirements is a reaction–diffusion equation,

$$\frac{\partial m}{\partial t} = R(m) + D\nabla^2 m = -\frac{\delta \mathcal{L}}{\delta m}, \qquad 8.$$

which describes the evolution of an order parameter m (for example, MSE) that takes different values in the two equilibrium states. The evolution of m is determined by a reaction term R that describes the tendency of m to evolve toward one of the equilibrium states, and a diffusion term $D\nabla^2 m$ that couples the evolution to the neighboring locations. The second equality in Equation 8 rewrites these terms as the functional derivative of a free energy,

$$\mathcal{L}(m) = \int_A \mathrm{d}\mathbf{x} \left[V(m) + |D\nabla^2 m|^2 \right], \qquad 9.$$

where $V(m)$ is a potential function satisfying $R(m) = -\delta V/\delta m$, and the integration is over an area A. Equation 8 shows that m will evolve in such a way as to minimize $\mathcal{L}$. The first term in $\mathcal{L}$ is reduced by increasing or decreasing m until it reaches one of the two equilibrium values (minima of V). This leaves large spatial gradients on the boundaries between the two phases, which contribute to the second term in $\mathcal{L}$. This contribution is reduced over time by growing and merging the regions with each phase and reducing the area occupied by their boundaries. The growth process can be shown to be characterized by dynamical self-similarity where the size of the features increases with time according to a power law. The end state that minimizes $\mathcal{L}$ will consist of two regions corresponding to the two equilibrium values of m. The length of the boundary will be as short as possible, for example, a circular blob of one phase.

There are several candidates for the physical processes responsible for self-aggregation (Section 2), but Craig & Mack (2013) and Windmiller & Craig (2019) have shown that several of them satisfy the generic requirements to produce coarsening. The first requirement is a feedback loop that causes moist (high-MSE) regions to get moister and dry (low-MSE) regions to get dryer. This could be associated with different radiative cooling rates in moist and dry regions (Section 3.1). Another mechanism arises through the entrainment of environmental air into cumulus clouds. In dry regions, this will inhibit the growth of the clouds since the mixing of dry air will lead to reevaporation of cloud water and a loss of buoyancy. The second requirement for coarsening is a process that couples neighboring regions in space. If the response of convection to large-scale gradients in environmental properties is stochastic, the variability will lead to a smoothing of the large-scale gradient on average, in a process analogous to molecular diffusion (Windmiller & Craig 2019). Triggering by spreading cold pools could lead to a similar effect.

It seems plausible that the atmosphere at times satisfies the conditions for coarsening, but the more important question is whether the characteristic behaviors of this process are observed. Most obviously, the final states in simulations of self-aggregation (e.g., **Figure 1*b***) are consistent with the requirement to minimize boundary length (Holloway & Woolnough 2016). The existence of a power law dependence of the length scale on time was investigated in large-domain simulations with periodic boundary conditions by Windmiller & Craig (2019), who indeed found the $t^{1/2}$ scaling predicted by Craig & Mack (2013) for the earlier stages of self-aggregation. Late in the simulations, however, the growth rate increased more rapidly, and Wing & Cronin (2016) found an exponent closer to 1 in simulations in a long, thin domain. These results suggest that different mechanisms for self-aggregation may be at work, even in idealized simulations.

3.3. The Effect of Cold Pools

Cold pools of air form under precipitating convective clouds when hydrometeors evaporate as they fall through unsaturated air. Previous work has shown that cold pools help trigger new convection in the vicinity of existing convective storms, leading to convective organization (Droegemeier & Wilhelmson 1987, Tompkins 2001b). Motivated by the observational and numerical evidence, a group of simple models have been constructed to simulate self-aggregation with parameterized effects of cold pools. Some of these models consider self-aggregation as self-organized criticality driven by cold pool dynamics.

Tompkins (2001b) discovered that cold pool edges were crucial in determining the positions of subsequent convective updrafts. Dynamically, cold pools can be distinguished from their surroundings by thin lines (**Figure 5*a*,*b***) of strong near-surface horizontal convergence (Haerter et al. 2019, Henneberg et al. 2020). Mechanical lifting at cold pool edges, especially under collisions of multiple cold pools (Droegemeier & Wilhelmson 1985, Torri et al. 2015, De Szoeke et al. 2017), can relatively quickly generate new convective updrafts. These results suggest that the locations of current rain cells and their cold pools determine the positions of subsequent rain cells—a causal replication mechanism is thereby encoded (Böing 2016, Haerter et al. 2019, Hirt et al. 2020).

The consequences of cold pool interactions on the organization of the convective cloud field as a whole are complex, and deciphering them is computationally costly when running simulations at sufficiently high resolution. Simplified modeling of the cold-pool-to-cold-pool replication chain has allowed researchers to highlight several organizing mechanisms. Single cold pool effects, where one cold pool gives rise to a new rain cell, have been implemented into GCM subgrid parameterizations (Rio et al. 2013). In a more conceptual, coarse-grained model, Windmiller (2017) described the effect of cold pools as introducing an enhanced triggering probability at sites close to previous cold pool centers, as well as an inhibition at the center itself. The clustering of cells under this mechanism can be mapped onto the directed percolation problem (Bröker

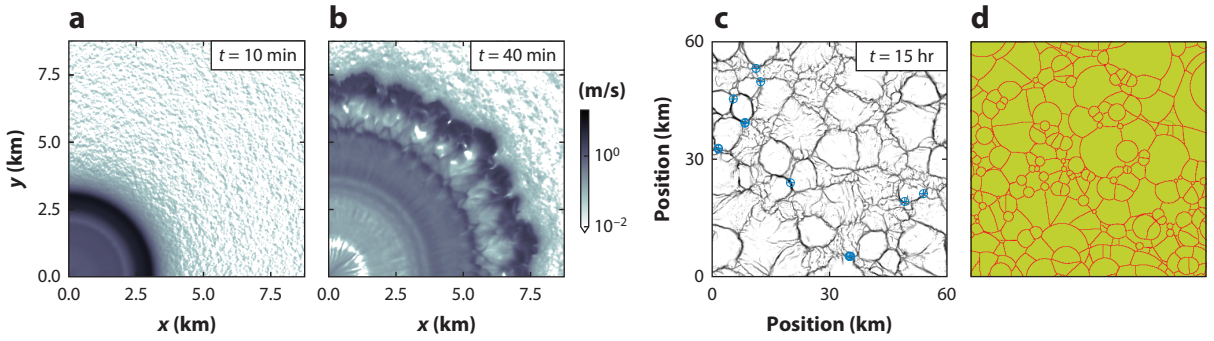

Figure 5

Cold pool spreading and collisions. (*a*,*b*) Horizontal cross sections of near-surface radial velocity (*a*) 10 min after initialization (note the initial axisymmetric structure) and (*b*) 40 min after initialization (note the formation of a lobe-and-cleft symmetry breaking along the cold pool's gust front). (*c*) Cold pool collisions during the diurnal cycle. (*d*) A conceptual model for cold pool gust front collisions. Panels *a* and *b* adapted with permission from Meyer & Haerter (2020). Panels *c* and *d* adapted with permission from Haerter et al. (2019); copyright 2019 American Geophysical Union.

& Grassberger 1999). The model qualitatively reproduces the spreading of convective activity observed in RCE simulations.

Organizing effects may be qualitatively different when the interactions among multiple cold pools are taken into account. In a two-layer model, Böing (2016) replaced the details of convective updrafts, downdrafts, and their interactions by a particle description, where each particle represents a unit of energy. In the spirit of self-organized criticality (Bak et al. 1987), an underlying lattice structure is assumed and discrete particles are allowed to populate this lattice. An excess number of particles in any given lattice box gives rise to an updraft. Subsequent downdrafts redistribute particles to surrounding lattice sites—thus acting to create a spatial imbalance of particles. When allowed to evolve, the model yields patterns reminiscent of those in large eddy simulations for cold pool gust fronts.

In an even more coarsely grained model, Haerter (2019) viewed the dynamical replication of cells in RCE as proportional to a nonlinear function of local rain cell number density $n(\mathbf{r})$, with the time dependence given by $\dot{n}(\mathbf{r}) = p_0(1-\overline{n})n(\mathbf{r})^m[1-n(\mathbf{r})] - f_\mathrm{d}\, n(\mathbf{r})$. Here, $\overline{n}$ is the domain-mean number density, $\mathbf{r}$ is the location vector, and p_0 and f_d are parameters describing interactions and decay, respectively. Imposing a global constraint on total cell number through the factor $1-\overline{n}$ and choosing $m = 2$, we see that the probability that a new cell occurs disproportionately increases with the cell number density in the surroundings, resulting in continuous transitions between (long-lived) clustered and (short-lived) featureless states. Hence, cold pool interactions together with a global constraint can—in principle—provide sustained self-aggregation.

In a recent parameter-free model for diurnal cycle convection (Haerter et al. 2019), cold pool gust fronts were simply assumed to evolve as circles with increasing radii and circle centers were taken to be initially positioned at random, using a 2D domain with periodic boundary conditions. Loci where two distinct circles, that is, gust fronts, met were considered a stationary front without further activity; loci where three circles met were taken as the origins of new circle centers—thus encoding a replication dynamics. Realizing that cells then occur in generations, the mean time Δt from one generation to the next goes as $\Delta t \sim \overline{n}^{-1/2}$ and the change in cell number is $\Delta\overline{n} \sim (r_\mathrm{p}-1)\overline{n}$, with r_p the probability of replication. It follows that such dynamics should lead to an approximately linear increase of typical scales with time, commensurate with LES simulation results (Haerter et al. 2017) (**Figure 5*c*,*d***). The model was further shown to induce the clustering of rain cells.

The cold pool collision mechanisms mentioned above all require a geometry where rain cells give birth to subsequent rain cells by cold pool collisions occurring between the locations of the rain cells. However, observational data suggest that large cold pools, such as those associated with mesoscale convective systems, can often trigger new rain cells autonomously, that is, near their outer edges (Houze 2004, Schumacher & Rasmussen 2020). Recent simulations suggest a process termed diurnal self-aggregation, within which mesoscale convective systems can emerge spontaneously when the spatial number density of rain cells is sufficiently high (Haerter et al. 2020). It was thereby found that combined cold pools of diameters $\mathcal{O}(100$ km) can autonomously form in the course of the diurnal cycle—given that the temperature forcing amplitude is sufficiently large.

3.4. Convection–Gravity Wave Interaction

Evidence from mechanism-denial experiments and from APE and MSE analyses points to the importance of the boundary layer (e.g., the lowest 2 km) to the development and maintenance of self-aggregation. Motivated by this, Yang (2021) constructed a linear shallow-water model that simulates the dynamics of the planetary boundary layer. This model successfully simulated the spontaneous development of self-aggregation and suggested that convectively coupled gravity waves can form standing wave packets, separating the domain into convectively active and inactive regions. This model only included a minimum set of ingredients in order to reproduce the basic features of a minimal simulation presented by Yang (2018a) in which radiative, surface-flux, vapor–buoyancy feedback loops and the evaporation of rain were both absent.

The governing equations of this shallow-water model are given by

$$\partial_t u = -\partial_x \phi - u/\tau_\mathrm{d}, \tag{10.}$$

$$\partial_t \phi + c^2 \partial_x u = F_\mathrm{c} + F_\mathrm{l} - (\phi - \bar{\phi})/\tau_\mathrm{d}, \tag{11.}$$

where u is horizontal velocity (m/s); ϕ is the geopotential ($\mathrm{m}^2/\mathrm{s}^2$), and $\bar{\phi}$ is its domain average; τ_d is a linear damping timescale (1/s); c is the gravity wave speed (m/s); F_c is convective heating ($\mathrm{m}^2/\mathrm{s}^3$), which is parameterized as a mass sink; and F_l represents large-scale forcings that are constant in time and space ($\mathrm{m}^2/\mathrm{s}^3$), parameterized as a mass source. In the model, the mass source represents processes that make the atmosphere more unstable; the mass sink represents processes that make the atmosphere more stable. The convective heating F_c is negative when convection is active; F_l is positive. At steady state, F_c balances F_l over the entire domain, reaching RCE.

Convection is parameterized as a triggered process. When ϕ exceeds a threshold ϕ_c, convection is triggered, and latent heat is released. Each convective event occupies a finite length ($2r_\mathrm{c}$) and lasts for a finite time (τ_c):

$$F_\mathrm{c} = -\frac{q}{r_\mathrm{c} \times \tau_\mathrm{c}} \times \left[1 - \left(\frac{\Delta t - \tau_\mathrm{c}/2}{\tau_\mathrm{c}/2}\right)^2\right] \times \left(1 - \frac{R^2}{R_\mathrm{c}^2}\right), \tag{12.}$$

where q measures the amplitude of convection (a positive number), Δt represents the time interval since the onset of convection, and r represents the distance of a location to the convective center. The term F_c is zero for $\Delta t > \tau_\mathrm{c}$ or $R > R_\mathrm{c}$. In the model, the forcing amplitude is small, so ϕ_c is approximately equal to the equilibrium geopotential, $\phi_\mathrm{e} \equiv c^2$. This is evident in our simulation results below. Therefore, choosing a gravity wave speed also determines the triggering threshold of convection.

In this shallow-water model, the fluid dynamics is linear and the only nonlinearity comes from the triggered convection. Therefore, the absolute amplitude of any forcing is not of interest. There are five free parameters: the convective timescale τ_c, the radius of convective storms r_c, the gravity

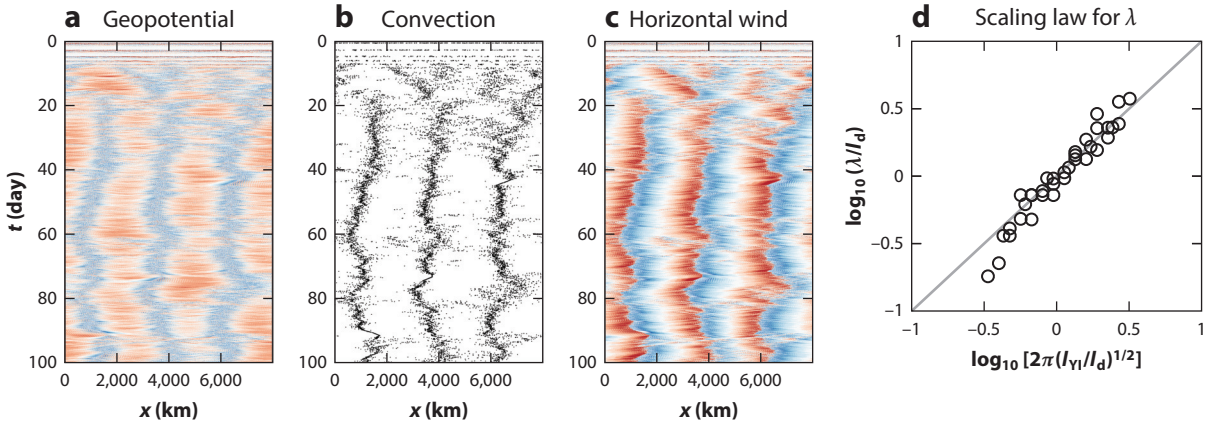

Figure 6

Shallow-water simulation results for the (*a*) geopotential, (*b*) convection, (*c*) horizontal wind, and (*d*) scaling law for the spatial scale of the aggregate λ. Red represents positive values, and blue represents negative values. Figure adapted with permission from Yang (2021); copyright 2021 American Meteorological Society.

wave speed c, the damping timescale τ_d, and the number density of convective events S_c. The last of these, S_c, is a derived parameter, measuring the number of convective events per unit area per time. Over a time period T and a spatial scale L, the energy balance is given by $n \times q \sim F_l \times T \times L$, where n represents the number of convective events over T and L. The parameter S_c then emerges from this energy balance: $S_c \equiv n/(T \times L) \sim F_l/q$. The integrated effect of an individual storm over its entire life cycle and convective area scales with q (Yang & Ingersoll 2013, 2014).

This shallow-water model can successfully simulate spontaneous organization of large-scale circulations and convection. **Figure 6*a–c*** shows the geopotential ϕ, convection, and the horizontal u for a simulation. Large-scale structures in convection and circulation self-emerge quickly, reaching a statistically steady state around day 30. Convective centers collocate with large-scale low-pressure centers and convergence, which is consistent with results in CRM simulations (see **Figure 2** of Yang 2018a). Within the large-scale envelopes, there are small-scale, short-lived gravity waves excited by convective storms. These gravity waves propagate toward opposite directions at the same speed, forming standing wave patterns that meander slowly. The standing wave pattern separates the domain into convectively active and inactive areas with a spatial scale of $\mathcal{O}$(1,000 km).

A fundamental question is what controls the spatial scale of self-aggregation, λ. Yang (2021) developed a scaling theory for λ by combining dimensional analysis and shallow-water simulations (**Figure 6*d***). He discovered that λ is set by two characteristic length scales in the model, $l_d = c \times \tau_d$ and $l_{YI} = \sqrt{c/S_c}$. Here l_d measures how far gravity waves can travel with linear damping, and l_{YI} measures how far gravity waves can travel without interfering with convective storms. The scaling relationship is given by

$$\lambda = 2\pi \left(l_d \cdot l_{YI}\right)^{1/2}. \qquad 13.$$

This scaling theory agrees well with a wide range of simulation results (**Figure 6*d***).

Yang & Ingersoll (2013, 2014) developed a rotating version of this shallow-water model, which can reproduce all basic features of the Madden–Julian oscillation (MJO; see the margin definition). This result echos an emerging view that the MJO is a form of self-aggregation over an equatorial β plane (see Section 4.4). This agreement between the shallow-water model and more comprehensive models may suggest that the triggered convection scheme of Yang (2021) might have captured key aspects of how convection interacts with atmospheric flows.

Madden–Julian oscillation (MJO): a month-long, planetary-scale rainfall pattern in the tropics

4. REAL-WORLD MANIFESTATIONS AND WHAT A SELF-AGGREGATION VIEWPOINT BRINGS TO THEM

Equilibrium climate sensitivity (ECS): the global mean equilibrium surface air temperature response to a doubling of CO_2

4.1. Inhomogeneous Surface

The SST (either mean or gradient) plays a critical role in the occurrence and progress of self-aggregation through its effects on surface fluxes (e.g., the WISHE effect discussed in Section 2.2). The mean SST affects the atmospheric water vapor and temperature profile and thus can potentially alter the mechanisms of self-aggregation. The dependency of self-aggregation on mean SST remains an open question (Wing et al. 2020).

When SST is inhomogeneous in space, but still fixed in time, the shallow circulation driven by SST gradients can also force or oppose the aggregation (here we refer to aggregation and not self-aggregation, as the simulations are no longer homogeneous; thus, the organization does not necessarily follow from self-organizing internal feedback loops, but can also be forced by SST gradients), in addition to the radiatively driven shallow circulation discussed in Section 2.1 (Tompkins 2001a, Shamekh et al. 2020b). Over the tropical regions, deep convective organizations are associated with long-persisting large-scale SST patterns rather than mean SST. SST patterns warm and moisten the boundary layer where the SST is higher, creating a pressure gradient and low-level flow (Back & Bretherton 2009).

Over a spherical domain in which the SST is temporally fixed but changes meridionally, in otherwise homogeneous conditions, Muller & Hohenegger (2020) have shown that there is a resemblance between their precipitation distribution and an Intertropical Convergence Zone (ITCZ). They confirm that a boundary layer convergence, primarily controlled by the SST gradient, drives the aggregation and leads to the formation of a precipitation band similar to an ITCZ, whereas in the zonal direction, the shallow circulation known from aggregation studies over homogeneous conditions acts to contract the convergence line.

Studies of SST patterns, although more realistic than constant SST studies, still exclude the interaction between the SST and the atmosphere. Considering short and small SST variability (such as surface cooling by cloud shading), an interactive SST is expected to prevent or delay self-aggregation. Indeed, over dry nonconvective regions, the SST warms due to enhanced short-wave radiation. The generated SST gradient drives a thermally driven shallow circulation that counteracts the radiatively driven one, thus preventing or delaying the self-aggregation (Hohenegger & Stevens 2016, Shamekh et al. 2020a). In this case, once the warm but dry region becomes moist again, convection emerges and suppresses the thermally driven circulation. The emergence of convection leads to the formation of a cold SST anomaly by cloud shading below the convective region. Grabowski (2006) has shown that the interplay between SST cooling in the convective region and SST warming in the nonconvective region, along with the fact that convection likes warmer surfaces, leads to the propagation of convective clusters, always following the warm SST anomaly.

Over land, the generation of a soil moisture gradient between precipitating and nonprecipitating regions leads to a homogenization of the precipitation field (Hohenegger & Stevens 2018). As over oceans with SST gradients, soil moisture gradients trigger circulation from cold and wet regions to dry and warm regions, which are opposed to the background convective circulation and act to disorganize the convection.

4.2. Climate Sensitivity

The increase of atmospheric CO_2 concentration leads to an increase of global temperature. The susceptibility of the earth to this forcing is quantified by the earth's equilibrium climate sensitivity (ECS). The effective climate sensitivity of the earth is expected to lie between 2.6 and 3.9 K with a 66% probability (Sherwood et al. 2020).

Khairoutdinov & Emanuel (2010) first discovered that the degree of convective aggregation could affect climate sensitivity because of its strong impact on top-of-atmosphere radiation balance. It was shown that self-aggregation is associated with a drying of the atmosphere in both simulations (Bretherton et al. 2005) and observations (Hohenegger & Jakob 2020). This drying allows more outgoing long-wave radiation to space, cooling the planet. Changes in the degree of convective aggregation with warming can thus feed back on the temperature, and models with distinct degrees of self-aggregation can have different ECS (Cronin & Wing 2017). Atmospheres with stronger self-aggregation are not only drier but also warmer and more stable, with decreased high-cloudiness and often increased low-level and mid-level cloudiness (Wing et al. 2020).

The RCE conceptualization provides an ideal framework to assess the effect of self-aggregation on climate sensitivity, which is currently being investigated in a multimodel ensemble (Becker & Wing 2020) using outputs from the RCEMIP (RCE Model Intercomparison Project) (Wing et al. 2018). As expected, an increase in self-aggregation with SST counteracts the warming and expresses itself as a lowering of the climate sensitivity. Preliminary results have shown that ECS does not depend on the mean degree of self-aggregation, only on its change.

Allowing the SST to interact with convection may drastically change the expected effect of self-aggregation on climate sensitivity, possibly negating its effect. In their GCM simulations, Coppin & Bony (2018) found that the negative feedback loop associated with enhanced aggregation with warming is offset by a positive feedback loop due to a reduction of low cloud cover. Low clouds are more sensitive to warming when SST gradients can develop, like in the case with an interactive SST, as they are restricted to the colder areas of the domain. Allowing the SST to interact also removes the nonmonotonic behavior of self-aggregation with SST, a result confirmed by Drotos et al. (2020) over a wider range of forcings.

The contribution of the feedback loops leading to self-aggregation in idealized simulations (Section 3) to observed convective aggregation, compared to other mechanisms such as land–sea contrasts, is still unknown. In observations, Tobin et al. (2012) found an increase in outgoing long-wave radiation in more aggregated mesoscale scenes, consistent with idealized simulations. They further found that this increase is largely compensated by a reduction in reflected short-wave radiation due to reduced low- and mid-level cloudiness. However, looking at the effect of convective aggregation on the radiation budget for the full tropics, Bony et al. (2020), in contrast, did find a correlation between variations in self-aggregation and the tropical radiation budget. Although using quite distinct approaches, Bony et al. (2020) and Becker & Wing (2020) in essence came to similar conclusions: Variability in self-aggregation and low cloud amount accounts for most of the variance in the radiation budget. This emphasizes the potential importance of convective aggregation for the climate.

4.3. Precipitation Extremes

Although the most studied implication of self-aggregation is its impact on the top-of-atmosphere radiative balance, it is also expected to affect rainfall. A starting point in understanding this is to recognize that in an RCE system, the domain- and time-averaged precipitation rate is approximately constrained by the requirement to conserve energy within the atmosphere (see the margin definition of "RCE" in Section 2.1). The power loss from radiation must be balanced by a gain from surface turbulent heat fluxes, and these surface fluxes are dominated by a latent heat of evaporation from ocean surfaces, which from water conservation equals precipitation. The above constraint means that self-aggregation can affect the average rain rate by altering the radiative cooling of the atmosphere. Self-aggregation robustly increases outgoing long-wave radiation to space, the net radiative cooling of the atmosphere, and the mean precipitation in simulated RCE states.

However, of greater interest is the possible impact of self-aggregation on the intensity of extreme rain events (Pendergrass 2020). The distribution of the instantaneous rain rate at a point in observations and simulations has an approximately exponential tail at high rain rates. Physically, these rates P_e are determined approximately by (O'Gorman & Schneider 2009, Fildier et al. 2018, Muller & Takayabu 2020)

$$P_e \approx -\epsilon\omega\widehat{\left.\frac{dq_s}{dp}\right|_{\theta_e^*}}, \qquad 14.$$

where $\widehat{(...)}$ denotes a mass-weighted vertical integral. The three factors on the right-hand side of Equation 14 denote the bulk precipitation efficiency ϵ, the vertical pressure velocity ω, and the vertical gradient of saturated specific humidity taken at constant saturation–equivalent potential temperature. The first, or microphysical, term is the fraction of expected condensation realized as surface precipitation, which depends on small-scale turbulent processes and the fate of condensed droplets and ice crystals. The second, or dynamic, term is the rate of pressure change due to vertical velocity. The third, or thermodynamic, term indicates the condensation expected per unit pressure reduction.

A key motivation for studies of extreme precipitation is its sensitivity to global warming (O'Gorman 2012). The base expectation is that extreme precipitation will increase at roughly 7% per degree Celsius owing to the well-known temperature dependence of the thermodynamic factor in Equation 14. However, the other two factors could amplify or diminish this scaling. In particular, global RCE simulations that showed increasing convective organization with warming also showed an increased climate scaling of P_e (Pendergrass et al. 2016). This is consistent with the increase of extreme rain with increasing organization (Bao et al. 2017), although its amplitude can depend on the model and scenario examined (Fildier et al. 2017, Pendergrass 2020).

Self-aggregation can impact hourly or daily precipitation extremes because of the persistence of convection in time and space that it entails (Colin et al. 2019, Masunaga & Mapes 2019). This persistence increases the maximum accumulation of rain over hourly or daily time intervals even though instantaneous rates may be unaffected (Bao & Sherwood 2019). This near-invariance of instantaneous rain statistics comes from a cancellation of changes in ω and ϵ: The reduced speed of updrafts offsets the enhancement of precipitation efficiency occurring in a locally moister environment (Tompkins & Semie 2017). This cancellation may depend on the model configuration, as recent studies report substantial effects of self-aggregation on instantaneous (N. Da Silva, S. Shamekh, C.J. Muller & B. Fildier, submitted manuscript) and hourly (Fildier et al. 2021) rain rates, mainly from increased precipitation efficiency.

4.4. Madden–Julian Oscillation

The MJO is a very large-scale [$\mathcal{O}$(10,000)-km east–west wavelength], low-frequency [$\mathcal{O}$(40-day) period] oscillation that manifests in the winds, water vapor, precipitation, and many other meteorological variables in the tropics. Although the MJO is one of the most important tropical weather systems, it was not discovered in observations until the early 1970s (Madden & Julian 1971) because it is most prominent over the tropical Indian and western Pacific Oceans, where data were very sparse in the presatellite era. Raymond (2001) was the first to suggest that the MJO is due to an instability in which cloud–radiation interactions play a key role.

Arnold & Randall (2015) were able to simulate the MJO using a multiphysics numerical model of the global atmosphere. The model set-up was highly idealized, with a global ocean of uniform SST and globally uniform incident solar radiation. The model was based on a version of the

Community Atmosphere Model of the National Center for Atmospheric Research, modified by replacing the conventional parameterized physics with an embedded CRM in each grid column of the global model (Khairoutdinov & Randall 2001). Arnold & Randall (2015) first performed a simulation without rotation. The results showed self-aggregation in the form of multiple convective clusters separated by dry regions, similar to the results obtained with CRMs on smaller domains. When rotation was switched on in a second simulation, the aggregated state took the form of an MJO centered on the equator, suggesting that the MJO is a form of self-aggregation that occurs on a rotating sphere.

More recently, Khairoutdinov & Emanuel (2018) obtained similar results in several numerical experiments, which revealed the roles of cloud–radiation interactions and surface fluxes in the growth and propagation of the MJO.

4.5. Tropical Cyclones

The feedback loops responsible for the self-aggregation of convection in nonrotating RCE have been found to be important for tropical cyclones in rotating RCE. The latter includes the effect of the earth's rotation through a nonzero Coriolis parameter f. As noted above, most studies mentioned in this review neglected the earth's rotation, i.e., they used $f = 0\ s^{-1}$. This is a reasonable approximation near the equator and at small scales, but it becomes questionable when the convective aggregate reaches mesoscales. At those scales, the effect of the earth's rotation starts to be appreciable.

In rotating RCE, one or several tropical cyclones develop, and both cold pools (Section 3.3) and radiative feedback loops (Section 3.1) have been found to significantly impact the genesis of the cyclone from homogeneous conditions (Davis 2015, Wing et al. 2016, Muller & Romps 2018). These results add to the growing literature on the importance of this phenomenon for the tropical atmosphere and suggest that self-aggregation, and the framework developed for its study, could help shed more light into the physical processes leading to cyclogenesis and cyclone intensification.

5. CONCLUDING REMARKS

The spectacular spontaneous self-aggregation of convective storms in idealized, homogeneous simulations has intrigued the community for decades (**Figure 1**). Numerical and theoretical studies have highlighted key processes, including radiation, cold pools, and gravity waves. Notably, the importance of low-tropospheric radiation and concomitant low-level circulation is widely recognized (Section 2). Given the nonlocality of radiative processes, mid-tropospheric drying can play a key role in enhancing low-tropospheric radiative cooling.

Overall, the analysis of instabilities in the tropical atmosphere that result from the coupling of radiative and convective heating to humidity perturbations (Section 3.1) remains a challenging research frontier. Current evidence from theoretical and modeling studies indicates that radiative–convective instabilities are likely in the tropical atmosphere, but their growth rates, spatial scales, and relevance to self-aggregation remain unclear.

Looking for evidence of self-aggregation in observations is further complicated by its slow evolution over weeks, leaving ample time for synoptic variability to disrupt the organization. One observation that appears robust is the two-peaked frequency distribution for humidity (e.g., Zhang et al. 2003), with intermediate moisture values comparatively scarce. This demonstrates the tendency of the tropical atmosphere to divide into wet and dry regions, but it provides no insight into their spatial organization. A recent paper by Beucler et al. (2020) goes some way toward bridging the gap between observation and theory. Beucler et al. showed that a direct correspondence holds

between the total length of the boundaries between moist and dry regions and an empirical free energy functional, both in RCE simulations and in the Atlantic ITCZ. Using this diagnostic they identified periods of increasing and decreasing aggregation on subseasonal and season timescales. While this does not provide decisive evidence that coarsening (Section 3.2) is occurring in the atmosphere, it clearly demonstrates how theoretical ideas lead to new insights into the observed behavior of the atmosphere.

Further work is needed to deepen understanding of the relative roles of surface fluxes versus rain reevaporation as sources of cold pool moistening, of the circumstances favoring mechanical versus thermodynamic triggering, of the relevance of multi–cold pool collisions (Section 3.3), and of the effect of cold pool dynamics on mid-tropospheric moistening and larger upscale organization, such as in mesoscale convective systems or convective self-aggregation. The latter has been shown to be hampered by relatively high (<2 km) horizontal model resolution (Yanase et al. 2020) and strong cold pools (Jeevanjee & Romps 2013). However, cold pool effects may become more acute as the model resolution is further increased (Meyer & Haerter 2020), thus raising the question of how convective self-aggregation can be made commensurate with cold pool–mediated organizing effects.

The various feedback loops leading to self-aggregation in the simple models of Section 3 raise the question of universality: Is there one universal process among all those described here? Is there overlap? Are those processes consistent or mutually exclusive? The complications of convection, radiation, and microphysics, typically parameterized in CRMs, are often neglected in simple models.

Bridging the gap between idealized models and observations requires investigating new metrics and more universal characterizations of organization (Windmiller & Craig 2019, Beucler et al. 2020) and directly testing its link to rainfall statistics (Tan et al. 2015, Roca & Fiolleau 2020, Semie & Bony 2020) despite the sparsity of measurements and the common modeling assumptions that do not systematically hold in reality—such as RCE or some parameterizations. Because rain intensity is one of the most commonly retrieved quantities in remote sensing, focusing on the links between aggregation and the spatiotemporal statistics of rain could also be a new interesting strategy to test various models and to assess the importance of self-aggregation in the real atmosphere.

Given the simplicity and idealized configurations of simulations where self-aggregation was first studied, its relevance to the real world is still debated. Increasingly many studies highlight the potential role of self-aggregation in many important geophysical phenomena, as reviewed in Section 4. Improved understanding of convective organization and its sensitivity to warming is hence a priority for climate science and climate model development in order to achieve accurate warming and rainfall projections in our current, and in a warming, climate.

DISCLOSURE STATEMENT

The authors are not aware of any biases that might be perceived as affecting the objectivity of this review.

ACKNOWLEDGMENTS

C.M. gratefully acknowledges funding from the European Research Council (ERC) under the European Union's Horizon 2020 research and innovation program (Project CLUSTER, grant agreement 805041). She also thanks Grand Équipement National de Calcul Intensif (GENCI), France, for providing access to their computing platforms at Très Grand Centre de Calcul (TGCC). J.O.H. gratefully acknowledges funding from the Villum Foundation (grant 13168), the ERC under the Horizon 2020 research and innovation program (grant 771859), and the Novo Nordisk

Foundation's Interdisciplinary Synergy Program (grant NNF19OC0057374). G.C. gratefully acknowledges the support of the transregional collaborative research center (SFB/TRR 165) "Waves to Weather" (**http://www.wavestoweather.de**) funded by the German Research Foundation (DFG). D.Y. is supported by a Packard Fellowship in Science and Engineering, the France–Berkeley Fund, Laboratory Directed Research and Development (LDRD) funding from the Lawrence Berkeley National Laboratory, and the US Department of Energy, Office of Science, Office of Biological and Environmental Research, Climate and Environmental Sciences Division, Regional and Global Climate Modeling Program under award DE-AC02-05CH11231.

LITERATURE CITED

Arnold NP, Putman WM. 2018. Nonrotating convective self-aggregation in a limited area AGCM. *J. Adv. Model. Earth Syst.* 10(4):1029–46

Arnold NP, Randall DA. 2015. Global-scale convective aggregation: implications for the Madden-Julian oscillation. *J. Adv. Model. Earth Syst.* 7(4):1499–518

Back LE, Bretherton CS. 2009. On the relationship between SST gradients, boundary layer winds, and convergence over the tropical oceans. *J. Climate* 22(15):4182–96

Bak P, Tang C, Wiesenfeld K. 1987. Self-organized criticality: an explanation of the 1/*f* noise. *Phys. Rev. Lett.* 59(4):381

Bao J, Sherwood SC. 2019. The role of convective self-aggregation in extreme instantaneous versus daily precipitation. *J. Adv. Model. Earth Syst.* 11(1):19–33

Bao J, Sherwood SC, Colin M, Dixit V. 2017. The robust relationship between extreme precipitation and convective organization in idealized numerical modeling simulations. *J. Adv. Model. Earth Syst.* 9(6):2291–303

Becker T, Wing AA. 2020. Understanding the extreme spread in climate sensitivity with the radiative-convective equilibrium model intercomparison project. *J. Adv. Model. Earth Syst.* 12:e2020MS002165

Beucler T, Cronin TW. 2016. Moisture-radiative cooling instability. *J. Adv. Model. Earth Syst.* 8:1620–40

Beucler T, Cronin TW, Emanuel KA. 2018. A linear response framework for radiative-convective instability. *J. Adv. Model. Earth Syst.* 10:1924–51

Beucler T, Leutwyler D, Windmiller JM. 2020. Quantifying convective aggregation using the tropical moist margin's length. *J. Adv. Model. Earth Syst.* 12(10):e2020MS002092

Böing SJ. 2016. An object-based model for convective cold pool dynamics. *Math. Clim. Weather Forecast.* 2:43–60

Bony S, Semie A, Kramer RJ, Soden B, Tompkins AM, Emanuel KA. 2020. Observed modulation of the tropical radiation budget by deep convective organization and lower-tropospheric stability. *AGU Adv.* 1:e2019AV000155

Bretherton CS, Blossey PN, Khairoutdinov M. 2005. An energy-balance analysis of deep convective self-aggregation above uniform SST. *J. Atmos. Sci.* 62(12):4273–92

Bröker HM, Grassberger P. 1999. SOC in a population model with global control. *Physica A* 267(3–4):453–70

Colin M, Sherwood S, Geoffroy O, Bony S, Fuchs D. 2019. Identifying the sources of convective memory in cloud-resolving simulations. *J. Atmos. Sci.* 76(3):947–62

Coppin D, Bony S. 2018. On the interplay between convective aggregation, surface temperature gradients, and climate sensitivity. *J. Adv. Model. Earth Syst.* 10(12):3123–38

Craig GC, Mack JM. 2013. A coarsening model for self-organization of tropical convection. *J. Geophys. Res.* 118(16):8761–69

Cronin TW, Emanuel KA, Molnar P. 2015. Island precipitation enhancement and the diurnal cycle in radiative-convective equilibrium. *Q. J. R. Meteorol. Soc.* 141(689):1017–34

Cronin TW, Wing AA. 2017. Clouds, circulation, and climate sensitivity in a radiative-convective equilibrium channel model. *J. Adv. Model. Earth Syst.* 9:2833–905

Davis CA. 2015. The formation of moist vortices and tropical cyclones in idealized simulations. *J. Atmos. Sci.* 72(9):3499–516

De Szoeke SP, Skyllingstad ED, Zuidema P, Chandra AS. 2017. Cold pools and their influence on the tropical marine boundary layer. *J. Atmos. Sci.* 74(4):1149–68

Droegemeier K, Wilhelmson R. 1985. Three-dimensional numerical modeling of convection produced by interacting thunderstorm outflows. Part I: control simulation and low-level moisture variations. *J. Atmos. Sci.* 42(22):2381–403

Droegemeier K, Wilhelmson R. 1987. Numerical simulation of thunderstorm outflow dynamics. Part I: outflow sensitivity experiments and turbulence dynamics. *J. Atmos. Sci.* 44(8):1180–210

Drotos G, Becker T, Mauritsen T, Stevens B. 2020. Global variability in radiative-convective equilibrium with a slab ocean under a wide range of CO_2 concentrations. *Tellus A* 72:1–19

Emanuel KA, Neelin JD, Bretherton CS. 1994. On large-scale circulations in convecting atmospheres. *Q. J. R. Meteorol. Soc.* 120(519):1111–43

Emanuel KA, Wing AA, Vincent EM. 2014. Radiative-convective instability. *J. Adv. Model. Earth Syst.* 6(1):75–90

Fildier B, Collins WD, Muller C. 2021. Distorsions of the rain distribution with warming, with and without self-aggregation. *J. Adv. Model. Earth Syst.* 13(2):e2020MS002256

Fildier B, Parishani H, Collins WD. 2017. Simultaneous characterization of mesoscale and convective-scale tropical rainfall extremes and their dynamical and thermodynamic modes of change. *J. Adv. Model. Earth Syst.* 9(5):2103–19

Fildier B, Parishani H, Collins WD. 2018. Prognostic power of extreme rainfall scaling formulas across space and time scales. *J. Adv. Model. Earth Syst.* 19(2):3252–67

Grabowski WW. 2006. Impact of explicit atmosphere–ocean coupling on MJO-like coherent structures in idealized aquaplanet simulations. *J. Atmos. Sci.* 63:2289–306

Grabowski WW, Moncrieff MW. 2004. Moisture–convection feedback in the tropics. *Q. J. R. Meteorol. Soc.* 130(604):3081–104

Haerter JO. 2019. Convective self-aggregation as a cold pool-driven critical phenomenon. *Geophys. Res. Lett.* 46(7):4017–28

Haerter JO, Berg P, Moseley C. 2017. Precipitation onset as the temporal reference in convective self-organization. *Geophys. Res. Lett.* 44:6450–59

Haerter JO, Böing SJ, Henneberg O, Nissen SB. 2019. Circling in on convective organization. *Geophys. Res. Lett.* 46(12):7024–34

Haerter JO, Meyer B, Nissen SB. 2020. Diurnal self-aggregation. *NPJ Clim. Atmos. Sci.* 3:30

Held IM, Hemler RS, Ramaswamy V. 1993. Radiative-convective equilibrium with explicit two-dimensional moist convection. *J. Atmos. Sci.* 50(23):3909–27

Henneberg O, Meyer B, Haerter JO. 2020. Particle-based tracking of cold pool gust fronts. *J. Adv. Model. Earth Syst.* 12(5):e2019MS001910

Herman MJ, Kuang Z. 2013. Linear response functions of two convective parameterization schemes. *J. Adv. Model. Earth Syst.* 5:510–41

Hirt M, Craig GC, Schäfer SA, Savre J, Heinze R. 2020. Cold-pool-driven convective initiation: using causal graph analysis to determine what convection-permitting models are missing. *Q. J. R. Meteorol. Soc.* 146(730):2205–27

Hohenegger C, Jakob C. 2020. A relationship between ITCZ organization and subtropical humidity. *Geophys. Res. Lett.* 47:e2020GL088515

Hohenegger C, Stevens B. 2016. Coupled radiative convective equilibrium simulations with explicit and parameterized convection. *J. Adv. Model. Earth Syst.* 8(3):1468–82

Hohenegger C, Stevens B. 2018. The role of the permanent wilting point in controlling the spatial distribution of precipitation. *PNAS* 115:5692–97

Holloway CE, Woolnough SJ. 2016. The sensitivity of convective aggregation to diabatic processes in idealized radiative-convective equilibrium simulations. *J. Adv. Model. Earth Syst.* 8(1):166–95

Houze RA Jr. 2004. Mesoscale convective systems. *Rev. Geophys.* 42(4):RG4003

Jeevanjee N, Romps DM. 2013. Convective self-aggregation, cold pools, and domain size. *Geophys. Res. Lett.* 40(5):994–98

Khairoutdinov MF, Emanuel K. 2018. Intraseasonal variability in a cloud-permitting near-global equatorial aquaplanet model. *J. Atmos. Sci.* 75(12):4337–55

Khairoutdinov MF, Emanuel KA. 2010. *Aggregated convection and the regulation of tropical climate*. Poster presented at the 29th Conference on Hurricanes and Tropical Meteorology, Tucson, AZ, May 13. **https://ams.confex.com/ams/29Hurricanes/techprogram/paper_168418.htm**

Khairoutdinov MF, Randall DA. 2001. A cloud resolving model as a cloud parameterization in the NCAR community climate system model: preliminary results. *Geophys. Res. Lett.* 28(18):3617–20

Khairoutdinov MF, Randall DA. 2003. Cloud resolving modeling of the ARM Summer 1997 IOP: model formulation, results, uncertainties, and sensitivities. *J. Atmos. Sci.* 60(4):607–25

Kiladis GN, Wheeler MC, Haertel PT, Straub KH, Roundy PE. 2009. Convectively coupled equatorial waves. *Rev. Geophys.* 47(2):RG2003

Kuang Z. 2010. Linear response functions of a cumulus ensemble to temperature and moisture perturbations and implications for the dynamics of convectively coupled waves. *J. Atmos. Sci.* 67(4):941–62

Kuang Z. 2018. Linear stability of moist convecting atmospheres. Part I: from linear response functions to a simple model and applications to convectively coupled waves. *J. Atmos. Sci.* 75:2889–907

Madden RA, Julian PR. 1971. Detection of a 40–50 day oscillation in the zonal wind in the tropical pacific. *J. Atmos. Sci.* 28(5):702–8

Mapes BE. 1993. Gregarious tropical convection. *J. Atmos. Sci.* 50(13):2026–37

Mapes BE. 2001. Water's two height scales: the moist adiabat and the radiative troposphere. *Q. J. R. Meteorol. Soc.* 127(577):2353–66

Masunaga H, Mapes BE. 2019. A mechanism for the maintenance of sharp tropical margins. *J. Atmos. Sci.* 77(4):1181–97

Meyer B, Haerter JO. 2020. Mechanical forcing of convection by cold pools: collisions and energy scaling. *J. Adv. Model. Earth Syst.* 12(11):e2020MS002281

Muller CJ. 2013. Impact of convective organization on the response of tropical precipitation extremes to warming. *J. Climate* 26:5028–43

Muller CJ. 2019. Clouds in current and in a warming climate. In *Fundamental Aspects of Turbulent Flows in Climate Dynamics: Lecture Notes of the Les Houches Summer School*, ed. F Bouchet, T Schneider, A Venaille, C Salomon, pp. 46–93. Oxford: Oxford Univ. Press

Muller CJ, Bony S. 2015. What favors convective aggregation and why? *Geophys. Res. Lett.* 42:5626–34

Muller CJ, Held IM. 2012. Detailed investigation of the self-aggregation of convection in cloud-resolving simulations. *J. Atmos. Sci.* 69:2551–65

Muller CJ, Romps DM. 2018. Acceleration of tropical cyclogenesis by self-aggregation feedbacks. *PNAS* 115(12):2930–35

Muller CJ, Takayabu Y. 2020. Response of precipitation extremes to warming: What have we learned from theory and idealized cloud-resolving simulations, and what remains to be learned? *Environ. Res. Lett.* 15(3):035001

Muller SK, Hohenegger C. 2020. Self-aggregation of convection in spatially varying sea surface temperatures. *J. Adv. Model. Earth Syst.* 12(1):e2019MS001698

O'Gorman PA. 2012. Sensitivity of tropical precipitation extremes to climate change. *Nat. Geosci.* 5(10):697–700

O'Gorman PA, Schneider T. 2009. The physical basis for increases in precipitation extremes in simulations of 21st-century climate change. *PNAS* 106:14773–77

Patrizio CR, Randall DA. 2019. Sensitivity of convective self-aggregation to domain size. *J. Adv. Model. Earth Syst.* 11(7):1995–2019

Pendergrass AG. 2020. Changing degree of convective organization as a mechanism for dynamic changes in extreme precipitation. *Curr. Clim. Change Rep.* 6(2):47–54

Pendergrass AG, Reed KA, Medeiros B. 2016. The link between extreme precipitation and convective organization in a warming climate: global radiative-convective equilibrium simulations. *Geophys. Res. Lett.* 43(21):11445–52

Pierrehumbert RT. 2010. *Principles of Planetary Climate*. Cambridge, UK: Cambridge Univ. Press

Raymond DJ. 2000. The Hadley circulation as a radiative-convective instability. *J. Atmos. Sci.* 57:1286–97

Raymond DJ. 2001. A new model of the Madden–Julian oscillation. *J. Atmos. Sci.* 58(18):2807–19

Raymond DJ, Sessions SL, Sobel AH, Fuchs Ž. 2009. The mechanics of gross moist stability. *J. Adv. Model. Earth Syst.* 1(3):9

Rio C, Grandpeix J-Y, Hourdin F, Guichard F, Couvreux F, et al. 2013. Control of deep convection by sub-cloud lifting processes: the ALP closure in the LMDZ5B general circulation model. *Clim. Dynam.* 40(9–10):2271–92

Roca R, Fiolleau T. 2020. Extreme precipitation in the tropics is closely associated with long-lived convective systems. *Commun. Earth Environ.* 1:18

Schumacher RS, Rasmussen KL. 2020. The formation, character and changing nature of mesoscale convective systems. *Nat. Rev. Earth Environ.* 1:300–14

Seidel SD, Yang D. 2020. The lightness of water vapor helps to stabilize tropical climate. *Sci. Adv.* 6(19):eaba1951

Semie AG, Bony S. 2020. Relationship between precipitation extremes and convective organization inferred from satellite observations. *Geophys. Res. Lett.* 47(9):e2019GL086927

Sessions SL, Sentić S, Herman MJ. 2016. The role of radiation in organizing convection in weak temperature gradient simulations. *J. Adv. Model. Earth Syst.* 8(1):244–71

Sethna JP. 2006. *Statistical Mechanics: Entropy, Order Parameters and Complexity*. Oxford: Oxford Univ. Press. 1st ed.

Shamekh S, Muller C, Duvel JP, d'Andrea F. 2020a. Self-aggregation of convective clouds with interactive sea-surface temperature. *J. Adv. Model. Earth Syst.* 12(11):e2020MS002164

Shamekh S, Muller C, Duvel JP, d'Andrea F. 2020b. How do ocean warm anomalies favor the aggregation of deep convective clouds? *J. Atmos. Sci.* 77(11):3733–45

Sherwood SC, Webb MJ, Annan JD, Armour KC, Forster PM, et al. 2020. An assessment of Earth's climate sensitivity using multiple lines of evidence. *Rev. Geophys.* 58(4):e2019RG000678

Sobel AH, Nilsson J, Polvani LM. 2001. The weak temperature gradient approximation and balanced tropical moisture waves. *J. Atmos. Sci.* 58:3650–65

Stevens B. 2005. Atmospheric moist convection. *Annu. Rev. Earth Planet. Sci.* 33:605–43

Tan J, Jakob C, Rossow WB, Tselioudis G. 2015. Increases in tropical rainfall driven by changes in frequency of organized deep convection. *Nature* 519(7544):451–54

Tobin I, Bony S, Roca R. 2012. Observational evidence for relationships between the degree of aggregation of deep convection, water vapor, surface fluxes, and radiation. *J. Climate* 25:6885–904

Tompkins AM. 2001a. On the relationship between tropical convection and sea surface temperature. *J. Climate* 14(5):633–37

Tompkins AM. 2001b. Organization of tropical convection in low vertical wind shears: the role of cold pools. *J. Atmos. Sci.* 58:1650–72

Tompkins AM, Semie AG. 2017. Organization of tropical convection in low vertical wind shears: role of updraft entrainment. *J. Adv. Model. Earth Syst.* 9(2):1046–68

Torri G, Kuang Z, Tian Y. 2015. Mechanisms for convection triggering by cold pools. *Geophys. Res. Lett.* 42(6):1943–50

Windmiller JM. 2017. *Organization of tropical convection*. PhD Thesis, Ludwig-Maximilians-Universität München, Munich, Ger.

Windmiller JM, Craig GC. 2019. Universality in the spatial evolution of self-aggregation of tropical convection. *J. Atmos. Sci.* 76(6):1677–96

Wing AA. 2019. Self-aggregation of deep convection and its implications for climate. *Curr. Clim. Change Rep.* 5(1):1–11. Erratum. 2019. *Curr. Clim. Change Rep.* 5(3):258

Wing AA, Camargo SJ, Sobel AH. 2016. Role of radiative-convective feedbacks in spontaneous tropical cyclogenesis in idealized numerical simulations. *J. Atmos. Sci.* 73(7):2633–42

Wing AA, Cronin TW. 2016. Self-aggregation of convection in long channel geometry. *Q. J. R. Meteorol. Soc.* 142(694):1–15

Wing AA, Emanuel KA. 2014. Physical mechanisms controlling self-aggregation of convection in idealized numerical modeling simulations. *J. Adv. Model. Earth Syst.* 6(1):59–74

Wing AA, Emanuel KA, Holloway C, Muller C. 2017. Convective self-aggregation in numerical simulations: a review. *Surv. Geophys.* 38:1173–97

Wing AA, Reed KA, Satoh M, Stevens B, Bony S, Ohno T. 2018. Radiative–convective equilibrium model intercomparison project. *Geosci. Model Dev.* 11:793–813

Wing AA, Stauffer CL, Becker T, Reed KA, Ahn M-S, Arnold NP, et al. 2020. Clouds and convective self-aggregation in a multimodel ensemble of radiative-convective equilibrium simulations. *J. Adv. Model. Earth Syst.* 12(9):e2020MS002138

Wood R. 2012. Stratocumulus clouds. *Mon. Weather Rev.* 140(8):2373–423

Yanase T, Nishizawa S, Miura H, Takemi T, Tomita H. 2020. New critical length for the onset of self-aggregation of moist convection. *Geophys. Res. Lett.* 47(16):e2020GL088763

Yang D. 2018a. Boundary layer diabatic processes, the virtual effect, and convective self-aggregation. *J. Adv. Model. Earth Syst.* 10(9):2163–76

Yang D. 2018b. Boundary layer height and buoyancy determine the horizontal scale of convective self-aggregation. *J. Atmos. Sci.* 75(2):469–78

Yang D. 2021. A shallow water model for convective self-aggregation. *J. Atmos. Sci.* 78(2):571–82

Yang D, Ingersoll AP. 2013. Triggered convection, gravity waves, and the MJO: a shallow-water model. *J. Atmos. Sci.* 70(8):2476–86

Yang D, Ingersoll AP. 2014. A theory of the MJO horizontal scale. *Geophys. Res. Lett.* 41(3):661–66

Yang D, Seidel SD. 2020. The incredible lightness of water vapor. *J. Climate* 33(7):2841–51

Zhang C, Mapes BE, Soden BJ. 2003. Bimodality in tropical water vapour. *Q. J. R. Meteorol. Soc.* 129:2847–66